Volume 8, Issue 3, 2019, 654 - 660 **ISSN 2284-6808**

Letters in Applied NanoBioScience

https://nanobioletters.com/

https://doi.org/10.33263/LIANBS83.654660

Original Research Article **Open Access Journal**

Received: 01.09.2019 / Revised: 14.09.2019 / Accepted: 16.09.2019 / Published on-line: 17.09.2019

On the perfect diameter condition to optimize the antibiotic nanoencapsulation: case of gramicidin

Guillaume Paris [1], and Fabien Picaud [1,*]

[1]Laboratoire de Nanomédecine, Imagerie et Thérapeutique, Université Bourgogne-Franche-Comté (UFR Sciences et Techniques), Centre Hospitalier Universitaire de Besançon, 16 route de Gray, 25030 Besançon, France

*corresponding author e-mail address: ***fabien.picaud@univ-fcomte.fr*** | Scopus ID: 820403200

ABSTRACT

In the present work, we propose to investigate the ionic transport mechanisms in a new optimized biomimetic system. Our studies performed using classical molecular dynamics simulations show that it was possible to optimize the geometry of a hydrophobic nanopore in order to stabilize a small antibiotic by confinement. The analyses of the antibiotic structure gathered with the free energy profiles of ion diffusion through the channel of the antibiotic demonstrate the stability and the functional encapsulation of the drug. It opens a new way to build biomimetic nanochannel or nanovector for drug delivery.

Keywords: *simulations; biomimetism; nanopore.*

1. INTRODUCTION

Biological ion channels are transmembrane proteins which have a crucial function in cellular activity [1-4]. Their major role is to regulate ionic permeability in cell membranes [5-7]. To realize correctly their function, they must be highly permeable to ions while selecting only one type of ions [5, 8-10]. If all the characteristics are gathered they can offer the unique natural way to both permeate and select ion with a very high rate. However, dysfunction may be the cause of many diseases [11-13].

Exceptional filtering properties of this kind of proteins have been adapted to the creation of highly competitive nanofilters. Indeed, nowadays the necessity to create increasingly competitive nanofilters meets an important need. The new nanobiofiltration domain, and in particular the separation processes, permits to meet many technological and industrial challenges [14-15]. We can quote, the sea water desalinization [16] or filtering ions like dialysis applications [17]. The main problem is to create high permeability nanofilters while keeping their selectivity and without an excessive energy intake [18-22].

On the other ways, the perfect conditions to encapsulate ionic channel need to develop specific hydrophobic nanopore whose structural properties can reproduce at most the biological media where the ionic channels are stable [23-24]. Recently, it has been proved that track-etched membrane can be functionalized adequately in order to create inside small nanopores whose radii can be modulated as a function of the awaiting properties [23]. The atomic layer deposition technique allows obtaining a perfect geometry inside the pore while the last trimethylsilanisation functionalization allows reproducing a strong hydrophobic media aims at stabilizing the transmembrane channel [25-27]. The quality and the control of the inner part of the nanopore could thus be managed and could yield to the creation of biomimetic nanopore when ionic channel will be translocated inside the nanopore. We can also imagine that the new biomimetic channel developed in this way could be used as a future cargo to transport the encapsulated drug until its target in order to repair or to ameliorate the current medical treatments [28-31].

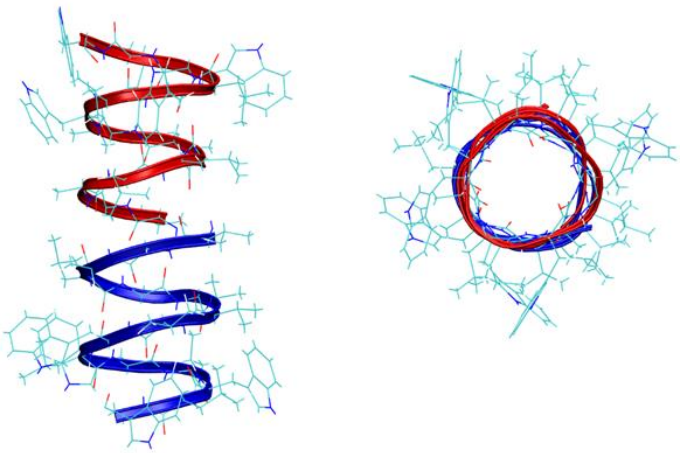

Figure 1. Side (left) and top (right) views of the gramicidin A dimer channel.

The development of high performing calculations allows now to study in global realistic view any system and to predict in a relatively low error the behavior of complex system. To limit the energy cost, a promising way is to confine biological channels directly inside a synthetic nanopore [32]. Recently, experiments have proved the feasibility of this kind of nanomembrane [32-33]. The difficulty of this method is that the protein must maintain its physiological functions in this new environment. Based on full atom molecular dynamics simulations, we study the role of the geometry on the encapsulation of a small protein channel with antibiotic properties, i.e. gramicidin [25]. In this monomeric form, the primary structure of the gramicidine A (gA) is a linear polypeptide of 15 hydrophobic amino acids. The conducting structure of gA is formed by two monomers of gA which have the capacity in lipid bilayers to create a head-head dimer by H-bonding between carbonyl oxygen and amino nitrogen of amino

acids terminals (Fig. 1) [34]. The gA channel so formed (with a radius lower than 0.5nm) is only permeable to monovalent cations (and water) and completely impermeable to divalent cations [35-37]. Stabilizing such a molecule inside solid state nanopore could lead to promised applications in drug vectorization as soon as the protein stabilization has been proved. It could also lead in selective permeable biomimetic nanopore with amazing properties.

The pore has been modeled according to the experiments. It was then modified geometrically in order to reproduce the known physical observables on the protein channel obtained in a biological membrane. Finally, the ultimate goal of our work is to retrieve the permeability and selectivity properties of the protein in an artificial environment. Since structure and function are closely linked for a protein, an important part of this work is devoted to the study of the stability of secondary and tertiary protein structures.

2. MATERIALS AND METHODS

a) Molecular dynamics simulations.

MD simulations were performed in the all-atom representation using NAMD_2.9b2 software [38] and the CHARMM 27 force field [39]. Equations of motion were integrated with a time step of 2 fs. Three-dimensional periodic boundary conditions were applied. Chemical bonds between hydrogen and heavy atoms were constrained to their equilibrium value with the SHAKE algorithm. NPT conditions were used in all simulations. To keep the temperature (300K) and the pressure (1 atm) constant, Langevin dynamics and Langevin piston method [40] were applied, respectively. For solvent, TIP3P model was used to describe water molecules. Concerning ions, parameters from Beglov and Roux [41-42] were taken into account for monovalent ions and from Marchand and Roux [43] for divalent ions. All simulations started from the same protein structure (RCSB Protein Data Bank ID code: 1JNO) [25]. The modeling of the biological system contained one gA channel and 72 DMPC lipids. The protein was solvated into a cubic box of about 40x40x150 $Å^3$ containing 1820 water molecules and Na^+ and Cl^- ions at concentration 0.15M (Figs 2a,b). The artificial complete system was constituted by one gA channel, 96 neopentane molecules assembled in a cylindrical like nanopore, Na^+ and Cl^- ions at concentration 0.15M and 3688 water molecules for a total of 21010 atoms and a periodic box of 35x35x140 $Å^3$(Figs 2c,d). The nanopore was then incorporated into a graphite bulk which was first open to let the pore inserting.

b) Free energy profiles calculations.

The free energy profiles were computed using the adaptive biasing force method [44], as implemented in NAMD [39]. In all ABF simulations, the reaction coordinate was the distance between the center of mass of the protein and the target ion, projected on the Cartesian *z*-axis (along the channel axis). The channel permeation pathway ($-12Å \le z \le 0Å$) was subdivided into four non-overlapping windows. Note that the second permeation pathway ($0Å \le z \le 12Å$) corresponds to the replica of the first one due to channel symmetry. The length of each window was 3.0 Å, in which MD was performed for 30 ns, resulting in a total simulation time of 120 ns. A 100 Kcal/mol/$Å^2$ boundary force constant was applied to restrain the motion of the ion of interest inside the window. Each window was sampled with a step size of 0.1 Å. The free energy profile was constructed by integrating the average force over all windows. The initial configurations for each window were taken from intermediate structures of MD simulations which have the target ion positioned near the next window. The biasing force was applied only after the accumulation of 1000 samples in a bin prior. During all ABF simulations, the motion of the target ion was limited to a cylinder of 8 Å on XY directions perpendicular to the axis of the protein.

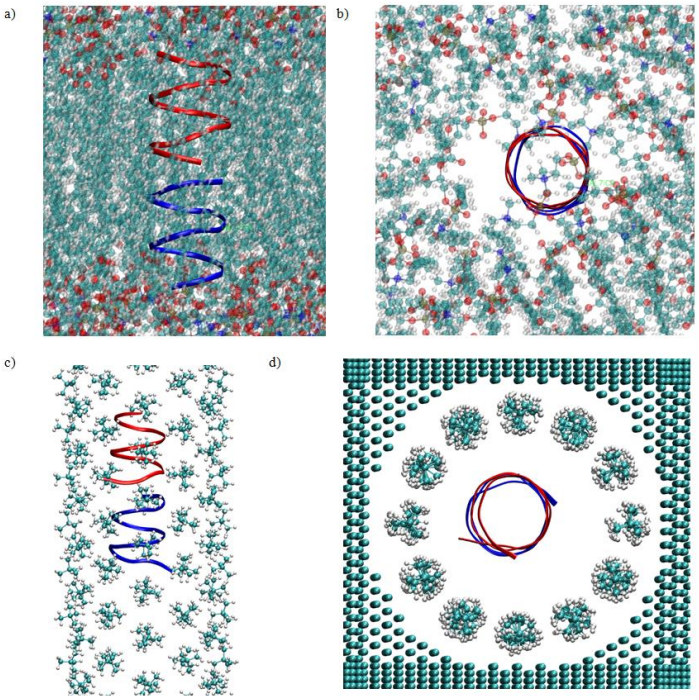

Figure 2. Complete system of simulation for the biological system (a) front and b) top views) and for the artificial system (c) front and d) top views). The gA was represented in two superimposed ribbon monomers of red and blue colors, DMPC lipids (blue), neopentane molecules (cyan) are represented in CPK mode. The NEOP nanopore is embedded in a graphite like solid in order to avoid any solvent departure away from the nanopore.

3. RESULTS

a) GA insertion. Recently [25] we demonstrated the possible encapsulation of gA inside hydrophobic solid state nanopore. Depending on the nanopore radius, the protein encapsulation can yield different behaviors leading to different stable states. At high nanopore radii, and low gA concentration, the hydrophobic inner wall of the nanopore is covered by the unfolded protein. Then, when the inner wall is completely covered (high gA concentrations), the proteins stabilized in the nanopore center. Due to the new confined environment made of unfolded protein, they kept their helical structure stable. In this case, the nanopore

properties were completely changed since it showed higher ionic permeability and selectivity proving the proper proteins insertion. In smaller nanopore radius, the accessible diameters should allow the protein keeping its stable structure. No further experimental work was performed on the perfect nanopore geometry in which gA could confine in stable position.

Indeed, using MD simulations, the pore diameter and structure can be modulated and optimized in order to avoid the unfolding of the protein. In this way, several diameters and two different nanopore forms were tested. First, we use carbon nanotubes where diameters ranged experimentally from several hundreds of nanometers up to 1.7 nanometers. However, whatever the tube radius tested in simulation we never obtained any stable protein backbone inside during the simulations. For each test, the protein progressively unfolded due to the small hydrophobic character of the inner pore wall as shown in Fig.3.

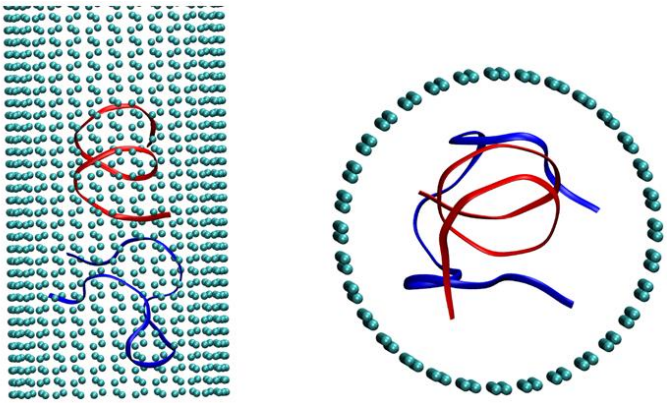

Figure 3. snapshot of the last stage of molecular dynamic simulation for gA encapsulation (ribbon representation in red and blue for the two gA monomers) in carbon (blue atom in CPK representation) nanotube of diameter 2.1 nm.

On the contrary, when studying nanopore made of neopentane molecular assembly, we observed for small diameters the ability of the protein to be stable inside. From the analysis of all the data, the diameter in which gA could leave its helix fold ranged between 1.7 to 2.3 nm. Hence, gA could be thus inserted in this narrowest drying nanopore. In this very high hydrophobic confined media, the role of the protein on the water behavior should be thus studied carefully in order to analyze further the ionic properties of the biomimetic nanopore. With liquid reservoir junctions, we observed that the water progressively filled the inner pore of the protein (hydrophilic nanochannel) [45], and also the hydrophobic nanopore. When the gA is inside the hydrophobic nanopore, its helical structure counterbalances the high hydrophobicity of the nanopore and forces the water molecules to be inside the nanopore as shown in [46].

b) Structural stability of ga

After the gA insertion and the good wetting of the nanopore, we have compared the structural stability of the protein in its biological environment and in the artificial one (Figures 4 a,b). A quick observation of the secondary structure along simulation time showed that globally the protein structure does not change anymore when it was held inside the synthetic nanopore. To quantify this, the root means square deviations (RMSD) were calculated for the protein backbone inside the biological membrane (Fig. 4a) or confined inside the nanopore (Fig. 4b).

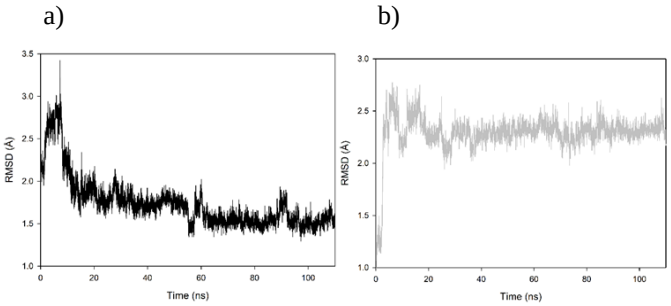

Figure 4. Root mean square deviation (RMSD) of the protein backbone with respect to the NMR structure 1JNO. The MD simulations were performed for gA both in this biological (a)) and solid-state (b)) environment.

The RMSD (Figures 4) were stabilized at the end of the simulation trajectory for the two systems. In the membrane cell, the structure of the protein was changed by only 1.2 Å from the reference structure. Very quickly in the trajectory of the protein in the artificial nanopore, the value of the RMSD converged to about 2.3 Å e. These 2 values can be considered as very close. The small difference was attributed to the mobility of the tryptophan residues located at the extremities of the protein. Their movements are more important in solid-state nanopore than in biological one due to their blockage by the lipid head in DMPC. These movements were also responsible for the evolution of the protein secondary structure. Indeed, the α-helix fraction evaluated through the STRIDE algorithm [47] implemented in VMD program [48] was stabilized at 82% in the biological media and only 62 % in the artificial nanopore. This small decrease is due to lack of confinement strength in solid state nanopore which allows the extremities of the protein to move in order to capture during the simulation monovalent ionic cations. Altogether, the dynamic pore wall seems to mimic at best the biological media and tend to stabilize the protein backbone.

To go further, we have analyzed for both systems the pair interaction energies between the gA and its environment. Two situations were particularly viewed since gA is mainly in contact with water in the two situations and with the lipid (or NEOP) molecules depending on the confined environment. The passage of ions through the inner part of the gA was not observed during enough time to be taken into account in this analysis. Figure 5a shows the pair interaction between gA and the lipid (or NEOP) molecules while Figure 5b depicts the pair interaction between the protein and the water molecules in both confined situations

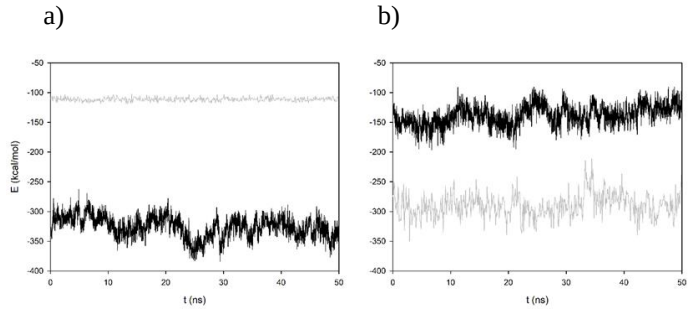

Figure 5. Pair interaction between protein and a) lipid or NEOP molecules and b) water. In black, pair interaction is showed for biological lipid environment and in gray, it concerns pair interaction in solid state NEOP nanopore.

From Fig. 5a we can observe that the pair interaction of the protein with the lipids is more favorable (-326 kcal/mol) than with the solid state molecules (-111 kcal/mol). Indeed, the labile environment of the biological membrane allows a complete optimization of the lipid positions around the protein while in the case of solid state molecules, the fixed central carbon atoms block any redistribution of the molecular position. This blockage is also directly observed in the fluctuations size of the pair interaction with the NEOP molecules which is negligible in solid state confinement while higher in lipid environment (around 25 kcal/mol). On the contrary, when analyzing the interaction with water, the tendency is inverted. In the NEOP nanopore, interactions between protein and water are lower (-290 kcal/mol) than in the lipid environment (-138 kcal/mol). Indeed, in lipid, no water molecule is present in this high hydrophobic media unlike the molecule in the protein channel while in the nanopore, we can add the contribution of the water molecules confined inside the NEOP nanopore that contribute to the interaction. Taking into account all the environmental contributions to the pair energies, gA felt a mean energy of -464 kcal/mol in lipid media while it reached -401 kcal/mol in the solid state nanopore. The difference is quite important but it allows, however, keeping the structure of the protein stable in the nanopore. Since the protein kept its structural stability, we can stand for good functioning with respect to the simulation time. To verify it, we have to check if the permeation properties of the artificial pore filled with the gA are of the same importance than in the biological media. The high permeability and selectivity upon monovalent cation diffusion should be retrieved in the functionalized nanopore. For this crucial point, we used free energy profiles calculations to have a better comprehension of the permeation mechanism.

c) Biomimetic system functioning.

We have investigated the permeation of ions for the biological and for the artificial system by calculating the Gibbs free energy profiles with respect to the distance along the Z-axis (Figure 6). We have limited the permeation pathway to one monomer only due to the symmetry of the system. The free energy profiles were calculated by the adaptive biasing force method for T=300 K starting from protein structures corresponding to their equilibrated structures. In a first time, we have chosen to evaluate the required energy for sodium and chlorine ions to cross the biological media.

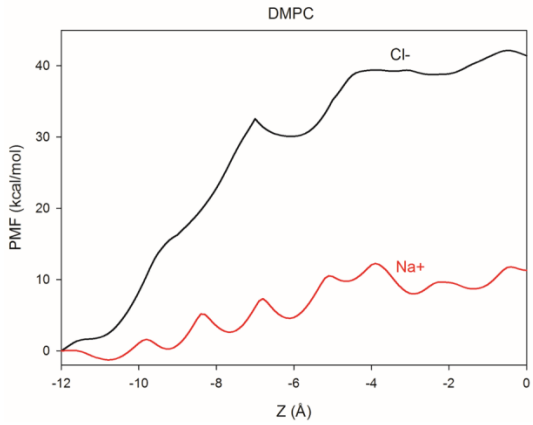

Figure 5. PMF curves obtained in DMPC membrane for Cl- (black) and Na+ (red) ions in one gA monomer.

The curves shown in Figure 5 are in agreement with the available data, particularly for Na+ ions [49-50] which is the main species that should translocate through the channel. It presents local minima located periodically along the channel as obtained in [49-50] and increases until an energy barrier equal to 12.5kcal/mol, while it reached around 11kcal/mol in the literature [50]. The minimum is obtained for us for the first energy well whereas in literature it is observed for the second one located at about -8.5 Å. These small differences could be due to a lack of sampling in our simulations or to different simulation parameters used in each study. Note that the same calculations were done on potassium ion in Ref. [51]. It shows an energy minimum at the entry of the channel and a progressive energy increase until its center. The barrier height was on the same order than the barrier observed here for sodium ion. When calculating the PMF for chloride ion, we can observe a continuous increase of the energy barrier along the pore axis which stabilized near the center of the dimer structure at around 40kcal/mol. Due to the high energy barrier, we can conclude with no doubt that the protein is completely selective for anion diffusion while letting the monovalent cation diffuse quite easily from one stable site to another one.

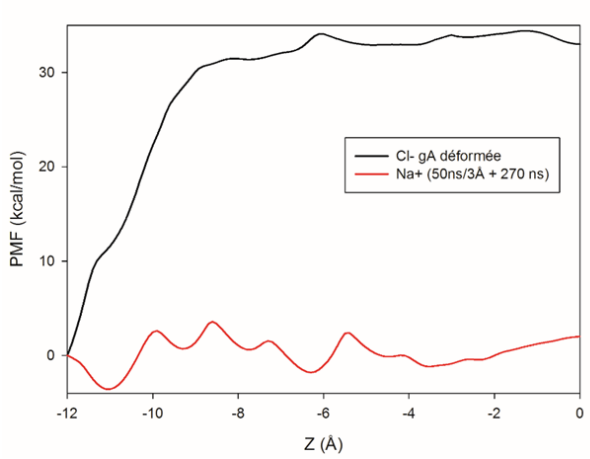

Figure 6. PMF curves obtained in NEOP membrane for Cl- (black) and Na+ (red) ions in one gA monomer.

The same calculations were then performed for gA encapsulated in the high hydrophobic solid state nanopore (Fig. 6). In this case, the anion still presented a continuous increasing energy barrier until 33 kcal/mol, while the monovalent cation showed a valley of potential energy which oscillated around -3.8 kcal/mol and 3.7 kcal/mol. We can thus deduce from these results that the protein kept its ability to block the anion while let diffusing quite easily the monovalent cation. To go further, we analyze and compare the different situations obtained in both DMPC or NEOP nanopore. Figure 7 depicts the comparison of both energy valleys for monovalent cation and anion respectively. It is clearly shown on this graph that the behavior of the protein towards the anion still not change anyway for the biologic or the hydrophobic media. Forcing the permeation of a chloride ion toward gA nanochannel in both DMPC or NEOP media would lead to similar behavior with energetic barriers of about 35-40kcal/mol. In the case of the hybrid membrane, the gA structure was deformed by the chloride ion permeation which resulted by conformational changes quantifiable by the RMSD. We could thus assume here that gA continues blocking anions and the biomimetic nanopore would result in anion selective properties.

On the other ways, the energy pathways for the sodium ion appear quite different. The energy barriers to overcome in the two cases are different. In the biological system, it reached about 12.5 kcal/mol while it was only 7.5 kcal/mol for the hybrid system. However, depending on the position of the cation, we retrieved for both media the positions of the minimums and of the maximums in the pathway. The energy differences can be explained by the small relaxation of the backbone structure at equilibrium which allows the sodium to diffuse more freely inside the nanochannel. Indeed, the RMSD of the backbone converged to 1.2Å in DMPC while it increased to 2.5Å in NEOP. Although very little higher, this modification of the structure would certainly lead to the decrease of the energy barrier for the monovalent ion that reached the nanochannel (cations and anions since these 2 species showed a decrease of the PMF values compared to the DMPC one). The Na^+ ions permeation through the synthetic membrane is fully possible. We can assume, like in biological environment that this behavior is generalizable to any monovalent cations. This indicates that the functioning of the gA is correct and that it kept its permeability.

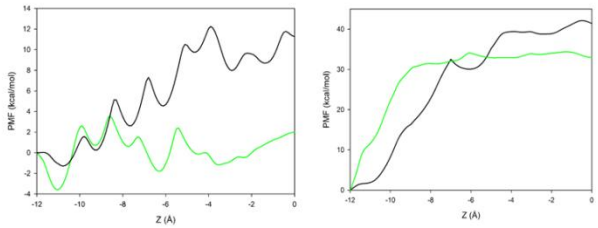

Figure 7. Gibbs free energy profile with respect to the distance along Z-axis for a sodium in left graph (chloride in right graph) ion calculated for the biological (black) and artificial (green) media.

We finally estimate the free energy profile for a divalent cation. We chose the magnesium cation and let him diffuse inside the encapsulated gramicidin channel. Results shown in Figure 8 are not in agreement with a perfect selectivity toward this kind of cation. As demonstrated before for calcium cation [51], the high selectivity of gA for these ions is depicted very rapidly by a strong increase of the potential of mean force valley at the entry of the protein channel (as for chloride ion). We definitively lost this selectivity regarding the obtained results here. The biomimetic nanopore functionalized by gA protein reproduces mainly the biological properties of the protein but fails in blocking divalent cations selectivity.

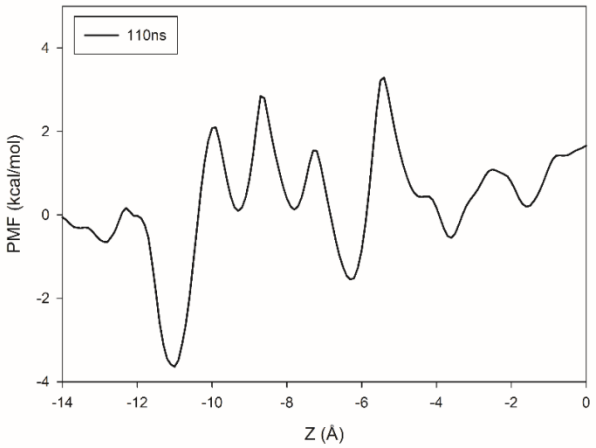

Figure 8. Gibbs free energy profile with respect to the distance along Z-axis for a magnesium ion calculated for the biological (black) and artificial (green) media.

4. CONCLUSIONS

In the present work, we proposed a new biomimetic system based on a solid-state hydrophobic nanoporous membrane and a confined gA in its biological form. After the successful insertion of gA in the synthetic nanopore, RMSD and global helicity of the protein confirmed the structural stability of the protein in this new medium. Permeability and selectivity properties have been verified by Gibbs free energy profiles calculations. Direct comparison of these profiles with those performed under biological conditions shows that gA keeps its filtration properties inside the nanopore. In particular, the passive diffusion of Na+ cations through the nanochannel is favored inside solid state nanopore as in biologic media. The energy barriers that cation should pass are lowered by about 40% due to the small modifications of the protein backbone structure. The complete anion selectively is however retrieved with a high entrance energy barriers ranging from 30 to 40 kcal/mol, even with the modified protein. This opens the possible development of ionic selective nanopump and proves the possibility for strong hydrophobic nanopore to stabilize drug protein in its inner volume in view of future biomimetic applications or drug vectorization.

5. REFERENCES

1. Almog, M.; Barkai, T.; Lampert, A.; Korngreen, A. Voltage-Gated Sodium Channels in Neocortical Pyramidal Neurons Display Cole-Moore Activation Kinetics. *Front Cell Neurosci* **2018,** *12*, 187-187, https://doi.org/10.3389/fncel.2018.00187.

2. Bernèche, S.; Roux, B. Energetics of ion conduction through the K+ channel. *Nature* **2001,** *414* (6859), 73-77, https://doi.org/10.1038/35102067.

3. Smart, O. S.; Breed, J.; Smith, G. R.; Sansom, M. S. A novel method for structure-based prediction of ion channel conductance properties. *Biophysical Journal* **1997,** *72* (3), 1109-1126, https://doi.org/10.1016/S0006-3495(97)78760-5.

4. Wang, J.; Ou, S.-W.; Wang, Y.-J. Distribution and function of voltage-gated sodium channels in the nervous system. *Channels (Austin)* **2017,** *11* (6), 534-554, https://doi.org/10.1080/19336950.2017.1380758.

5. Chen, X.-Z.; Vassilev, P. M.; Basora, N.; Peng, J.-B.; Nomura, H.; Segal, Y.; Brown, E. M.; Reeders, S. T.; Hediger, M. A.; Zhou, J. Polycystin-L is a calcium-regulated cation channel permeable to calcium ions. *Nature* **1999,** *401* (6751), 383-386, https://doi.org/10.1038/43907.

6. O'Connell, A. M.; Koeppe, R. E.; Andersen, O. S. Kinetics of gramicidin channel formation in lipid bilayers: Transmembrane monomer association. *Science* **1990,** *250*, 1256, https://doi.org/10.1126/science.1700867.

7. Smirnov, S. N.; Vlassiouk, I. V.; Lavrik, N. V. Voltage-Gated Hydrophobic Nanopores. *ACS Nano* **2011,** *5* (9), 7453-7461, https://doi.org/10.1021/nn202392d.

8. Clatot, J.; Hoshi, M.; Wan, X.; Liu, H.; Jain, A.; Shinlapawittayatorn, K.; Marionneau, C.; Ficker, E.; Ha, T.; Deschênes, I. Voltage-gated sodium channels assemble and gate

as dimers. *Nature Communications* **2017,** *8* (1), 2077, https://doi.org/10.1038/s41467-017-02262-0.
9. Compoint, M.; Picaud, F.; Ramseyer, C.; Girardet, C. Zip gating of the KcsA channel studied by targeted molecular dynamics. *Chemical Physics Letters* **2005,** *407* (1), 199-204, https://doi.org/10.1016/j.cplett.2005.03.087.
10. Domene, C.; Bond, P. J.; Sansom, M. S. P. Membrane Protein Simulations: Ion Channels And Bacterial Outer Membrane Proteins. In *Advances in Protein Chemistry*, Academic Press: 2003; Vol. 66, pp 159-193, https://doi.org/10.1016/S0065-3233(03)66005-5.
11. Compoint, M.; Carloni, P.; Ramseyer, C.; Girardet, C. Molecular dynamics study of the KcsA channel at 2.0-Å resolution: stability and concerted motions within the pore. *Biochimica et Biophysica Acta (BBA) - Biomembranes* **2004,** *1661* (1), 26-39, https://doi.org/10.1016/j.bbamem.2003.11.019.
12. Compoint, M.; Picaud, F.; Ramseyer, C.; Girardet, C. Targeted molecular dynamics of an open-state KcsA channel. *The Journal of Chemical Physics* **2005,** *122* (13), 134707, https://doi.org/10.1063/1.1869413.
13. Kadala, A.; Charreton, M.; Charnet, P.; Cens, T.; Rousset, M.; Chahine, M.; Vaissière, B. E.; Collet, C. Voltage-gated sodium channels from the bees Apis mellifera and Bombus terrestris are differentially modulated by pyrethroid insecticides. *Scientific Reports* **2019,** *9* (1), 1078, https://doi.org/10.1038/s41598-018-37278-z.
14. Marchetti, P.; Peeva, L.; Livingston, A. The Selectivity Challenge in Organic Solvent Nanofiltration: Membrane and Process Solutions. *Annual Review of Chemical and Biomolecular Engineering* **2017,** *8* (1), 473-497, https://doi.org/10.1146/annurev-chembioeng-060816-101325.
15. Siria, A.; Poncharal, P.; Biance, A. L.; Fulcrand, R.; Blase, X.; Purcell, S. T.; Bocquet, L. Giant osmotic energy conversion measured in a single transmembrane boron nitride nanotube. *Nature* **2013,** *494* (7438), 455-458, https://doi.org/10.1038/Nature11876.
16. Shannon, M. A.; Bohn, P. W.; Elimelech, M.; Georgiadis, J. G.; Marinas, B. J.; Mayes, A. M. Science and technology for water purification in the coming decades. *Nature* **2008,** *452* (7185), 301-310, https://doi.org/10.1038/nature06599.
17. Bontha, J. R.; Pintauro, P. N. Water Orientation and Ion Solvation Effects during Multicomponent Salt Partitioning in a Nafion Cation-Exchange Membrane. *Chem Eng Sci* **1994,** *49* (23), 3835-3851, https://doi.org/Doi 10.1016/0009-2509(94)00205-3.
18. Briggs, K.; Madejski, G.; Magill, M.; Kastritis, K.; de Haan, H. W.; McGrath, J. L.; Tabard-Cossa, V. DNA Translocations through Nanopores under Nanoscale Preconfinement. *Nano letters* **2018,** *18* (2), 660-668, https://doi.org/10.1021/acs.nanolett.7b03987.
19. Pevarnik, M.; Healy, K.; Davenport, M.; Yen, J.; Siwy, Z. S. A hydrophobic entrance enhances ion current rectification and induces dewetting in asymmetric nanopores. *Analyst* **2012,** *137* (13), 2944-2950, https://doi.org/10.1039/C2an16139g.
20. Picaud, F.; Kraszewski, S.; Ramseyer, C.; Balme, S.; Dejardin, P.; Janot, J. M.; Henn, F. Enhanced potassium selectivity in a bioinspired solid nanopore. *Physical Chemistry Chemical Physics* **2013,** *15* (45), 19601-19607, https://doi.org/10.1039/c3cp52123k.
21. Shen, Y.-x.; Song, W.; Barden, D. R.; Ren, T.; Lang, C.; Feroz, H.; Henderson, C. B.; Saboe, P. O.; Tsai, D.; Yan, H.; Butler, P. J.; Bazan, G. C.; Phillip, W. A.; Hickey, R. J.; Cremer, P. S.; Vashisth, H.; Kumar, M. Achieving high permeability and enhanced selectivity for Angstrom-scale separations using artificial water channel membranes. *Nature Communications* **2018,** *9* (1), 2294, https://doi.org/10.1038/s41467-018-04604-y.
22. Wang, P.; Wang, M.; Liu, F.; Ding, S.; Wang, X.; Du, G.; Liu, J.; Apel, P.; Kluth, P.; Trautmann, C.; Wang, Y. Ultrafast ion sieving using nanoporous polymeric membranes. *Nature Communications* **2018,** *9* (1), 569, https://doi.org/10.1038/s41467-018-02941-6.
23. Balme, S.; Picaud, F.; Manghi, M.; Palmeri, J.; Bechelany, M.; Cabello-Aguilar, S.; Abou-Chaaya, A.; Miele, P.; Balanzat, E.; Janot, J. M. Ionic transport through sub-10 nm diameter hydrophobic high-aspect ratio nanopores: experiment, theory and simulation. *Scientific Reports* **2015,** *5*, 10135, https://doi.org/10.1038/srep10135.
24. Lepoitevin, M.; Ma, T.; Bechelany, M.; Janot, J.-M.; Balme, S. Functionalization of single solid state nanopores to mimic biological ion channels: A review. *Advances in Colloid and Interface Science* **2017,** *250*, 195-213, https://doi.org/10.1016/j.cis.2017.09.001.
25. Bonhenry, D.; Kraszewski, S.; Picaud, F.; Ramseyer, C.; Balme, S.; Janot, J. M.; Henn, F. Stability of the gramicidin-A channel structure in view of nanofiltration: a computational and experimental study. *Soft Matter* **2011,** *7* (22), 10651-10659, https://doi.org/ 10.1039/C1SM06277H.
26. Borsley, S.; Cockroft, S. L. In Situ Synthetic Functionalization of a Transmembrane Protein Nanopore. *ACS Nano* **2018,** *12* (1), 786-794, https://doi.org/10.1021/acsnano.7b08105.
27. Cabello-Aguilar, S.; Abou Chaaya, A.; Bechelany, M.; Pochat-Bohatier, C.; Balanzat, E.; Janot, J. M.; Miele, P.; Balme, S. Dynamics of polymer nanoparticles through a single artificial nanopore with high-aspect-ratio. *Soft Matter* **2014,** *10*, 8413-8419, https://doi.org/10.1039/c4sm00392f.
28. El Khalifi, M.; Bentin, J.; Duverger, E.; Gharbi, T.; Boulahdour, H.; Picaud, F. Encapsulation capacity and natural payload delivery of an anticancer drug from boron nitride nanotube. *Physical Chemistry Chemical Physics* **2016,** *18* (36), 24994-25001, https://doi.org/10.1039/C6CP01387B.
29. El Khalifi, M.; Duverger, E.; Boulahdour, H.; Picaud, F. Theoretical study of the interaction between carbon nanotubes and carboplatin anticancer molecules. *Analytical Methods* **2015,** *7* (24), 10145-10150, https://doi.org/10.1039/C5AY00748H.
30. El Khalifi, M.; Duverger, E.; Gharbi, T.; Boulahdour, H.; Picaud, F. Theoretical demonstration of the potentiality of boron nitride nanotubes to encapsulate anticancer molecule. *Physical Chemistry Chemical Physics* **2015,** *17* (44), 30057-30064, https://doi.org/10.1039/C5CP05148G.
31. El Khalifi, M.; Duverger, E.; Gharbi, T.; Boulahdour, H.; Picaud, F. Theoretical use of boron nitride nanotubes as a perfect container for anticancer molecules. *Analytical Methods* **2016,** *8* (6), 1367-1372, https://doi.org/10.1039/C5AY02822A.
32. Balme, S.; Janot, J. M.; Berardo, L.; Henn, F.; Bonhenry, D.; Kraszewski, S.; Picaud, F.; Ramseyer, C. New Bioinspired Membrane Made of a Biological Ion Channel Confined into the Cylindrical Nanopore of a Solid-State Polymer. *Nano Letters* **2011,** *11*, 712-716, https://doi.org/10.1021/la902417m.
33. Vlassiouk, I.; Park, C.-D.; Vail, S. A.; Gust, D.; Smirnov, S. Control of Nanopore Wetting by a Photochromic Spiropyran: A Light-Controlled Valve and Electrical Switch. *Nano Letters* **2006,** *6* (5), 1013-1017, https://doi.org/10.1021/nl060313d.
34. Basu, I.; Chattopadhyay, A.; Mukhopadhyay, C. Ion channel stability of Gramicidin A in lipid bilayers: Effect of hydrophobic mismatch. *Biochimica et Biophysica Acta (BBA) -*

Biomembranes **2014,** *1838* (1, Part B), 328-338, https://doi.org/10.1016/j.bbamem.2013.10.005.
35. Diamanti, E.; Gutiérrez-Pineda, E.; Politakos, N.; Andreozzi, P.; Rodriguez-Presa, M. J.; Knoll, W.; Azzaroni, O.; Gervasi, C. A.; Moya, S. E. Gramicidin ion channels in a lipid bilayer supported on polyelectrolyte multilayer films: an electrochemical impedance study. *Soft Matter* **2017,** *13* (47), 8922-8929, https://doi.org/10.1039/C7SM01539A.
36. Kelkar, D. A.; Chattopadhyay, A. The gramicidin ion channel: A model membrane protein. *Biochimica et Biophysica Acta (BBA) - Biomembranes* **2007,** *1768* (9), 2011-2025, https://doi.org/10.1016/j.bbamem.2007.05.011.
37. Wenzel, M.; Rautenbach, M.; Vosloo, J. A.; Siersma, T.; Aisenbrey, C. H. M.; Zaitseva, E.; Laubscher, W. E.; van Rensburg, W.; Behrends, J. C.; Bechinger, B.; Hamoen, L. W. The Multifaceted Antibacterial Mechanisms of the Pioneering Peptide Antibiotics Tyrocidine and Gramicidin S. *mBio* **2018,** *9* (5), e00802-18, https://doi.org/10.1128/mBio.00802-18.
38. Phillips, J. C.; Braun, R.; Wang, W.; Gumbart, J.; Tajkhorshid, E.; Villa, E.; Chipot, C.; Skeel, R. D.; Kalé, L.; Schulten, K. Scalable molecular dynamics with NAMD. *Journal of Computational Chemistry* **2005,** *26* (16), 1781-1802, https://doi.org/10.1002/jcc.20289.
39. MacKerell, A. D.; Bashford, D.; Bellott; Dunbrack, R. L.; Evanseck, J. D.; Field, M. J.; Fischer, S.; Gao, J.; Guo, H.; Ha, S.; Joseph-McCarthy, D.; Kuchnir, L.; Kuczera, K.; Lau, F. T. K.; Mattos, C.; Michnick, S.; Ngo, T.; Nguyen, D. T.; Prodhom, B.; Reiher, W. E.; Roux, B.; Schlenkrich, M.; Smith, J. C.; Stote, R.; Straub, J.; Watanabe, M.; Wirkiewicz-Kuczera, J.; Yin, D.; Karplus, M. All-Atom Empirical Potential for Molecular Modeling and Dynamics Studies of Proteins *The Journal of Physical Chemistry B* **1998,** *102* (18), 3586-3616, https://doi.org/10.1021/acs.chemrev.8b00630.
40. Feller, S. Constant pressure molecular dynamics simulation: The Langevin piston method. *J. Chem. Phys.* **1995,** *103* (11), 4613, https://doi.org/10.1063/1.470648.
41. Beglov, D.; Roux, B. Finite representation of an infinite bulk system: Solvent boundary potential for computer simulations. *The Journal of Chemical Physics* **1994,** *100* (12), 9050-9063, https://doi.org/10.1063/1.466711.
42. Yoo, J.; Wilson, J.; Aksimentiev, A. Improved Model of Hydrated Calcium Ion for Molecular Dynamics Simulations Using Classical Biomolecular Force Fields. *Biopolymers* **2016,** *105*, 752-763, https://doi.org/10.1002/bip.22868.
43. Marchand, S.; Roux, B. Molecular dynamics study of calbindin D9k in the apo and singly and doubly calcium-loaded states. *Proteins: Structure, Function, and Bioinformatics* **1998,** *33* (2), 265-284, https://doi.org/10.1002/(sici)1097-0134(19981101)33:2.
44. Comer, J.; Gumbart, J. C.; Hénin, J.; Lelièvre, T.; Pohorille, A.; Chipot, C. The Adaptive Biasing Force Method: Everything You Always Wanted To Know but Were Afraid To Ask. *The Journal of Physical Chemistry B* **2015,** *119* (3), 1129-1151, https://doi.org/10.1021/jp506633n.
45. Xu, F.; Wei, M.; Zhang, X.; Song, Y.; Zhou, W.; Wang, Y. How Pore Hydrophilicity Influences Water Permeability? *Research* **2019,** *2019*, 10, https://doi.org/10.1155/2019/2581241.
46. Abou Chaaya, A.; Le Poitevin, M.; Cabello-Aguilar, S.; Balme, S.; Bechelany, M.; Kraszewski, S.; Picaud, F.; Cambedouzou, J.; Balanzat, E.; Janot, J.-M.; Thami, T.; Miele, P.; Dejardin, P. Enhanced Ionic Transport Mechanism by Gramicidin A Confined Inside Nanopores Tuned by Atomic Layer Deposition. *The Journal of Physical Chemistry C* **2013,** *117* (29), 15306-15315, https://doi.org/10.1021/jp403330d.
47. Frishman, D.; Argos, P. Knowledge-based protein secondary structure assignment. *Proteins: Structure, Function, and Bioinformatics* **1995,** *23* (4), 566-579, https://doi.org/10.1002/prot.340230412.
48. Humphrey, W.; Dalke, A.; Schulten, K. VMD - Visual Molecular Dynamics. *J. Molec. Graphics* **1996,** *14*, 33-38. , https://doi.org/10.1016/0263-7855(96)00018-5.
49. Liu, Z.; Xu, Y.; Tang, P. Steered Molecular Dynamics Simulations of Na+ Permeation across the Gramicidin A Channel. *The Journal of Physical Chemistry B* **2006,** *110* (25), 12789-12795, https://doi.org/10.1021/jp060688n.
50. Mustafa, M.; Busath, D. The Gramicidin Channel Ion Permeation Free-Energy Profile: Direct and Indirect Effects of CHARMM Force Field Improvements. *Interdisciplinary sciences, computational life sciences* **2009,** *1*, 113-27, https://doi.org/10.1007/s12539-009-0025-3.
51. Giorgino, T.; De Fabritiis, G. A High-Throughput Steered Molecular Dynamics Study on the Free Energy Profile of Ion Permeation through Gramicidin A. *Journal of Chemical Theory and Computation* **2011,** *7* (6), 1943-1950, https://doi.org/10.1021/ct100707s.

6. ACKNOWLEDGEMENTS

Computations have been performed on the supercomputer facilities of the Mesocentre of the University of Franche-Comté. They were also performed thanks to HPC resources from the Occigen supercomputer through the project A0010710123.